Image Instability Evaluation and Motion Correction for High-resolution MRI of the Rat Retina

X. Zhang[1], Y. Li[1], and T. Q. Duong[2]

[1]Yerkes National Primate Research Center, Emory University, Atlanta, GA, United States, [2]Research Imaging Center, University of Texas Health Science Center at San Antonio, San Antonio, TX, United States

Introduction High-resolution layer-specific retinal MRI is more susceptible to animal and hardware instability compared to typical brain MRI [1]. This study systemically examined these potential animal and hardware issues, and implemented solutions to maximize stability for high-resolution structural, physiological and functional MRI of the rat retina. Studies were performed on phantoms and the *in vivo* retinas to distinguish between potential animal and hardware issues. Solutions to maximize retinal MRI stability and post-processing displacement corrections are detailed. These solutions are expected to help set the stage for future retinal MRI studies.

Methods. Animal preparation: Retinal MRI was performed on adult Sprague-Dawley rats (300-350 g) under 1.1-3.0% isoflurane with pancuronium bromide (3 mg/kg first dose, 1 mg/kg/hr, ip) and mechanical ventilation. For anatomical MRI, rats were injected intravitreally with a small (2 µl) amount of Gd-DTPA 4 hours before MRI to enhance contrast. **Inhalation stimuli:** hyperoxic (100% O_2) and hypercapnic (5% CO_2, 21% O_2, balance N_2). **MRI methods:** Anatomical MRI (Bruker 7T) scanner was used with a gradient-recalled echo (GRE), TR= 150 ms, TE=3.5 ms, one 0.5-mm thick slice, 32 repetitions, spectral width (SW) = 26 kHz, matrix = 256x256, and FOV = 6.4x6.4 mm (25x25 µm). Blood-flow MRI was acquired using the CASL technique with four-shot, gradient-echo EPI, SW = 200 kHz, FOV = 11.5x11.5 mm, matrix = 128x128 (90x90 microns), slice thickness = 1.5 mm, TR = 3.0 s per segment, and TE = 14 ms. **B_o-drift correction:** A shift in the image space is a phase shift in the Fourier space described by $f(t-t_o) \quad \Leftrightarrow \quad e^{-i\omega t_o} \cdot F(\omega)$, where t is time, ω is the frequency, F is the image, and the double arrow is the Fourier transform. The image displacement can be corrected if the phase shift can be accurately estimated. The optimal phase correction was obtained by minimization of the difference in root-mean squares between the test image and a reference image. B_o drift correction was processed in image space[2]. Quantitative comparisons were made among the original uncorrected data, data corrected by image co-registration using SPM [www.fil.ion.ucl.ac.uk/spm] and data corrected by phase (B_o) drift. The following analyses were performed for comparison: *i)* temporal phase evolutions of the readout and phase-encode directions, *ii)* intensities of the spatial profiles of the images, *iii)* MRI signal time courses, *iv)* averaged anatomical and blood-flow images, *v)* the standard deviations of temporal EPI signal intensities of the retina divided by the mean (SD/mean) to evaluate temporal signal stability, and *vi)* baseline blood flow, and blood-flow changes associated with hypercapnic challenges.

Results. ***Phantom data:*** **Figure 1** plots the time course of the "phase" drifts expressed in pixel numbers and in microns from the conventional gradient-echo images at 25x25 µm and the profiles of before and after correction. EPI at 90x90 µm resolution (**Figure 2**) was processed as same as the gradient-echo images. ***In vivo* retina data:** ***Gradient-echo MRI*** acquisition at 25x25 µm shows appreciable displacement along the PE direction evidently but much less along the RO direction (**Figure 3A**). Averaging the original data without correction resulted in a loss of layer resolution as depicted by the spatial profiles across the retinal thickness (**Figure 3B**) and the averaged anatomical images (**Figure 3C**). Image co-registration and phase correction successfully removed the displacement error, resulting in improved laminar resolution. ***Echo-planar imaging:*** Phase drifts with EPI acquisition were generally more severe than that of the gradient-echo acquisition. **Figure 4B** shows the time courses of the interleaved non-labeled and labeled image intensities of the blood-flow measurements. The original data showed substantial drift in signal intensities and partially corrupted alternating non-labeled and labeled signal intensities due to image displacement. Image co-registration or phase correction removed the displacement error and improved blood-flow contrast, with the phase correction performed better. The signal time courses also showed robust BOLD (non-labeled images) and blood-flow increases associated with 5% CO_2 inhalation. **Figure 4C** shows the averaged blood-flow images of the original data, after co-registration, and after phase correction obtained during baseline (air) from one animal. Without correction, the blood-flow image erroneously appeared to show two layers of blood flow.

Discussion. Systemic paralysis successfully eliminates eye movement, as confirmed by optical imaging of the corneal surface. But appreciable B_o field drift is present at high-resolution MRI and it causes significant displacement error up to a few pixels over 8 minutes. This was independently confirmed as B_o frequency drift using localized ^1H_2O spectroscopy, and we conclude that temperature-related B_o drift is the dominant source of this spatial displacement likely. Phase corrections effectively removed such B_o field drift and displacement error for high-resolution retinal MRI.

Conclusions: This study systematically evaluated the source of instability for high-resolution layer-specific anatomical, physiological and functional MRI of the retina, and established solutions to reliably maximize stability. Substantial B_o drift and displacement error were in both conventional gradient-echo and EPI acquisitions can be corrected with post-processing. Some of these solutions may also be applicable to other high-resolution MRI studies in general.

References: 1) Cheng et al, PNAS, 103:17525-17530 2) Kochunov et al, JMRI, 12:956-959.

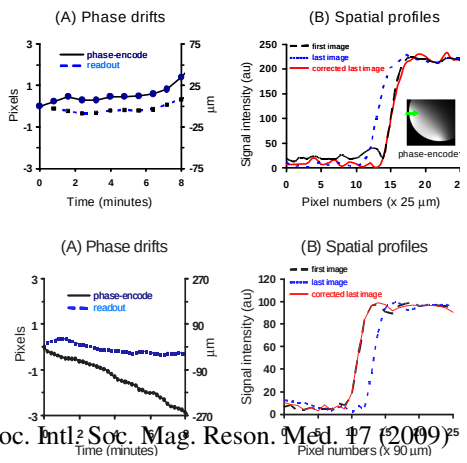

Figure 1. Phantom FLASH at 25 x 25 µm image shift with time (A) and profiles of the first image and last image and corrected last image (B)

Figure 2. Phantom EPI at 90x90µm image shift with time (A) and profiles of the first image and last image and corrected last image (B)

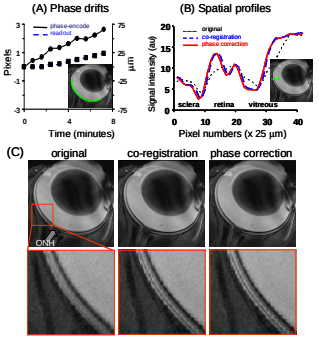

Figure 3. *In vivo* MRI of retina at 25 x 25 µm. A: temporal image shift, B: intensity profile, C: averaged images

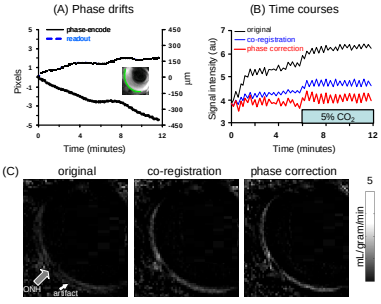

Figure 4. blood flow(BF) of retina by CASL at 90x90µm under CO2 challenge. A: temporal image shift B:ASL data with/without correction C: BF maps